Renewable Energy xxx (2010) 1–10

Contents lists available at ScienceDirect

Renewable Energy

journal homepage: www.elsevier.com/locate/renene

Ratios of UV, PAR and NIR components to global solar radiation measured at Botucatu site in Brazil

João F. Escobedo [a], Eduardo N. Gomes [a], Amauri P. Oliveira [b,*], Jacyra Soares [b]

[a] Department of Natural Resources, UNESP, Botucatu, São Paulo, Brazil
[b] Department of Atmospheric Sciences, IAG, USP, São Paulo, São Paulo, Brazil

ARTICLE INFO

Article history:
Received 17 April 2008
Accepted 15 June 2010
Available online xxx

Keywords:
Ultraviolet radiation
Photosynthetically active radiation
Near infrared solar radiation
Global solar radiation
Brazil

ABSTRACT

The relationships between the four radiant fluxes are analyzed based on a 4 year data archive of hourly and daily global ultraviolet (I_{UV}), photosynthetically active-PAR (I_{PAR}), near infrared (I_{NIR}) and broadband global solar radiation (I_G) collected at Botucatu, Brazil. These data are used to establish both the fractions of spectral components to global solar radiation and the proposed linear regression models. Verification results indicated that the proposed regression models predict accurately the spectral radiant fluxes at least for the Brazilian environment. Finally, results obtained in this analysis agreed well with most published results in the literature.

1. Introduction

Solar radiation transmitted through the earth's atmosphere has three primary streams of incoming radiant fluxes depending on their wavelength range: (i) The ultraviolet component (spectral range: 0.29–0.4 μm) is the high energetic portion of the solar spectrum; it is absorbed by ozone layer and other atmospheric constituents. This component has deleterious effects in many biological systems; disrupts proteins, causes skin cancer, eye cataract and other destructive effects in plants and materials [1–5]. (ii) The spectral PAR segment covering both photon and energy terms lies between 0.4 and 0.7 μm or 0.380–0.7 μm in the solar spectrum [6]. This spectral portion is used by plant biochemical processes in photosynthesis and it is important in most agricultural research [7–10]. (iii) The near infrared-NIR portion lies between 0.7 and 2.8 μm; it is applied to remote satellite techniques for retrieving total atmospheric water vapor column [11]. The NIR solar component is less investigated in comparison with the UV and PAR spectral solar segments [12,13].

One practical way to estimate UV, PAR and NIR is using empirical expressions derived from the correlation between global solar radiation (G) and its spectral components. The major advantage of empirical expressions is that they are simple to use and depend only on the global solar radiation at the surface, i.e., the most widely available data for solar radiation worldwide. However, empirical expressions have to be validated for the specific site using in situ measurements.

Simultaneous observations of UV, PAR, NIR and G are not frequently monitored and therefore most of the empirical expressions for estimating PAR [13–24] and UV [25–35] are independently derived through broadband solar component G. On the other hand, information on the relationship between radiant fluxes NIR and G is rather scarce [11,12,36].

In Brazil, most of the observational works available in the literature is based on broadband measurements of global and diffuse components of solar radiation at the surface [37–42]. Empirical expressions of PAR in terms of G can be found in ~~Refs.~~ [43,44]. Assunção and Escobedo [45] explored the relationship between UV and G for the area of Botucatu (Brazil).

To fill out the observational gap existing in Brazil, the Radiometric Station of São Paulo State University (Fig. 1) located in the city of Botucatu, Brazil, has carried out simultaneously measurements of UV and NIR components of the solar radiation spectrum and global solar radiation at the surface, continuously since 2001. It is the first time, in Brazil that measurements of UV and NIR were carried out simultaneously to global solar radiation.

The objective of this work is to explore the seasonal evolution of UV, PAR and NIR components of the solar radiation spectrum at the surface and to describe the development and validation of a set of linear regression models to estimate hourly and daily values of UV,

* Corresponding author. Tel.: + 55 11 3091 4701; fax: + 55 11 3091 4714.
E-mail address: apdolive@usp.br (A.P. Oliveira).

0960-1481/$ – see front matter © 2010 Elsevier Ltd. All rights reserved.
doi:10.1016/j.renene.2010.06.018

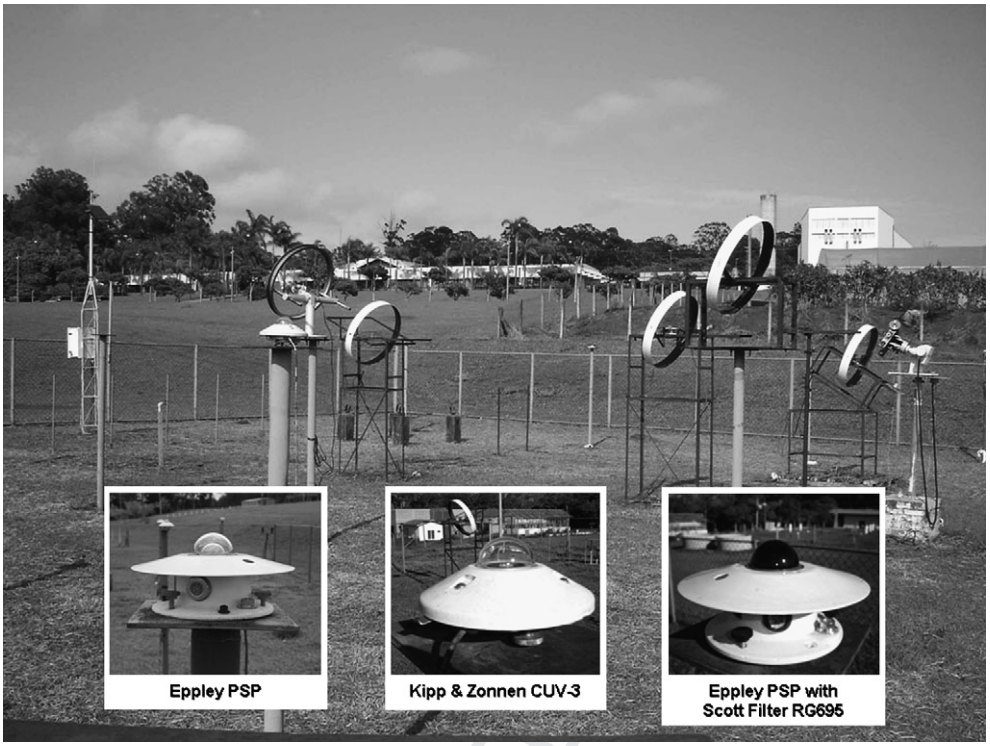

Fig. 1. Radiometric Station in Botucatu, State of São Paulo, Brazil. View of the NW quadrant.

PAR and NIR components of the solar radiation spectrum in terms of hourly and daily values of G observed at the surface. In this work the corresponding hourly and daily PAR values are indirectly estimated through values of UV, NIR and G radiant components.

The climate of Botucatu and the observations used in this work are described in Section 2. Section 3 presents the results and discussion and the conclusions are given in Section 4.

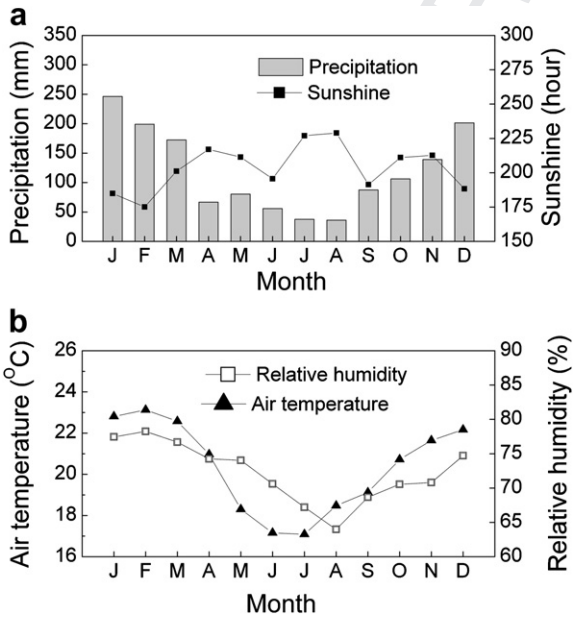

Fig. 2. Seasonal evolution of the monthly average values of (a) precipitation and sunshine hours and (b) air temperature and relative humidity at Botucatu. Precipitation and sunshine hours correspond to monthly accumulated values. Observations carried out during 30 years, from 1970 to 2000.

2. Site and measurements

The radiometric and meteorological stations (Fig. 1) are located in the rural area of Botucatu, in the School of Agronomic Sciences, State University of São Paulo (22.85°S, 48.45°W, 786 m above MSL).

Summer in Botucatu city is warm and wet while winter is mild cold and dry. The duration of the longest day is 13.4 h occurring in December. The duration of the shortest day is 10.6 h and it occurs in June. The highest number of sunshine hours (229.0) and the lowest number of sunshine hours (175.1) are observed in August and February, respectively. The highest amount of monthly accumulated precipitation (260.7 mm) is in January, in contrast to August, in which accumulated precipitation averages 38.2 mm. February is the hottest month of the year and July is the coldest one. Monthly air temperature ranges between 23.2 °C and 17.1 °C. February is the wettest month of the year and August is the driest one. Monthly average relative humidity values are 78.2% and 61.8%, respectively (Fig. 2).

The global solar irradiance, I_G (0.295–2.800 μm) on a horizontal plane was measured by an Eppley PSP model (Newport, Rhode Island, USA). The global ultraviolet irradiance, I_{UV} (0.290–0.400 μm), was measured with a Kipp & Zonen model CUV-3 (Delft, The Netherlands), whereas the global NIR component, I_{NIR} (0.695–2.800 μm) was measured with an Eppley PSP model equipped with a Schott glass filter 0.695–2.800 μm. This filter enables solar irradiance to be determined in the spectral range of 0.695–2.800 μm. Following the manufacture recommendation the calibration factor used in the filtered pyranometer was multiplied by 0.92 to correct effects of filter transmission on the sensor (Table 1).

All values of photosynthetically active solar irradiance (I_{PAR}) used in this work were indirectly estimated: $I_{PAR} = I_G - (I_{UV} + I_{NIR})$. Most published experimental PAR results are given in photobiological units (μE m^{-2} s^{-1} or μmol $m^{-2}s^{-1}$) [6]. In this analysis, the PAR component is expressed in W m^{-2} for irradiance and in MJ m^{-2} for both hourly and daily values.

Please cite this article in press as: Escobedo João F, et al., Ratios of UV, PAR and NIR components to global solar radiation measured at Botucatu site in Brazil, Renewable Energy (2010), doi:10.1016/j.renene.2010.06.018

Table 1
Pyranometer main features.

Feature	Global	Ultraviolet	Near infrared
Manufacturer	Eppley	Kipp and Zonen	Eppley
Calibration factor	7.45 μV $W^{-1}m^2$	312 μV $W^{-1}m^2$	8.12 μV $W^{-1}m^2$
Spectral Range	0.295–2.800 μm	0.290–0.400 μm	0.695–2.800 μm
Response time	1 s	5 ms	2 s
Linearity	±0.5% (0–2800 W m^{-2})	<1%	±1% (0–700 W m^{-2})
Cosine effect	±1% ($0° < Z < 70°$) ± 3% ($70° \leq Z < 80°$)	< ± 10%	± 5%
Temperature response	±1% (−20 °C–40 °C)	< ± 0.1%/K	±1% (−20 °C–40 °C)

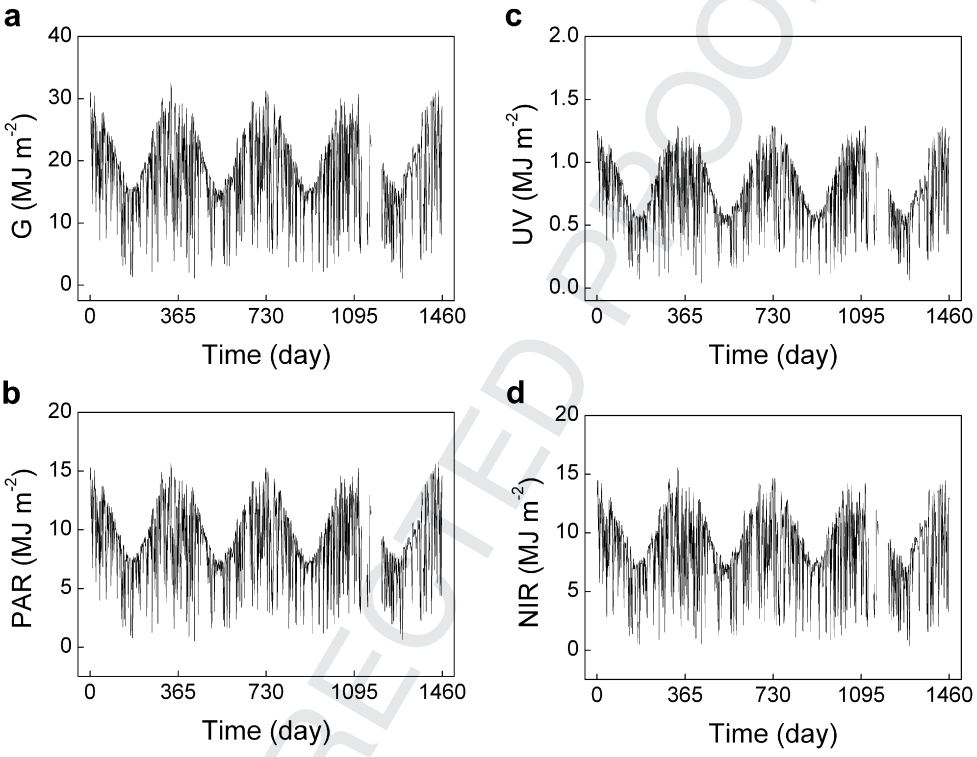

Fig. 3. Temporal evolution of daily values of (a) G, (b) PAR, (c) UV and (d) NIR radiation components observed at the surface in Botucatu from 2001 to 2004.

The uncertainty in the PAR values is of the order of 19% and it was estimated by error propagation considering the combination of 2% of uncertainty in the global, 15% of UV [46] and 2% of NIR sensors in the spectral range of 0.295–2800 μm, 0.295–0.400 μm and 0.695–2800 μm, respectively. The uncertainty in the pyranometer PSP Eppley, a secondary standard, was estimated experimentally by Ref. [47].

From 2001 to 2005 these three pyranometers were operating continuously. The 5 min average values of all irradiances were obtained, with a Campbell Datalogger data acquisition system, model CR23X, using measurements sampled with frequency of 1 Hz.

Calibration of solar radiation sensors was performed every 2 years using the procedures recommended by the WMO [40,41,48].

This work is based on observations carried out in Botucatu from 2001 to 2005. For the purpose of developing the empirical expressions to estimating spectral UV, PAR and NIR solar components, the radiometric data for 2001–2004 were used. Verification results of the derived empirical regression models were performed through radiant fluxes data obtained during 2005.

The dataset was inspected and suspicious values were removed from the series. Here, the data inspection was performed as an interactive process involving setting typical values characterizing the diurnal and seasonal evolution of G, UV, PAR and NIR. A climate

Table 2
Statistical properties of hourly values of G, UV, PAR and NIR observed between 2001 and 2004 in Botucatu.

Period	Radiation component	Fraction of global (%)	Mean (MJ m^{-2})	Standard deviation (%)	Maximum (MJ m^{-2})	Number of hours
2001	G	–	1.92	51.32	4.13	3265
	UV	4.17	0.08	51.02	0.17	3265
	PAR	48.96	0.94	50.95	2.05	3265
	NIR	46.88	0.90	51.94	1.97	3265
2002	G	–	1.86	51.04	4.14	3153
	UV	4.30	0.08	50.74	0.18	3153
	PAR	48.92	0.91	51.09	2.03	3153
	NIR	46.77	0.87	51.29	1.97	3153
2003	G	–	1.87	51.27	4.05	3273
	UV	4.28	0.08	51.41	0.18	3273
	PAR	48.66	0.91	51.57	2.04	3273
	NIR	46.52	0.87	51.32	1.88	3273
2004	G	–	1.78	55.14	4.12	2878
	UV	4.49	0.08	54.64	0.17	2878
	PAR	50.00	0.89	56.14	2.18	2878
	NIR	46.07	0.82	55.04	1.86	2878

Please cite this article in press as: Escobedo João F, et al., Ratios of UV, PAR and NIR components to global solar radiation measured at Botucatu site in Brazil, Renewable Energy (2010), doi:10.1016/j.renene.2010.06.018

Table 3
Statistical properties of daily values of G, UV, PAR and NIR observed between 2001 and 2004 in Botucatu.

Period	Radiation component	Fraction of global (%)	Mean (MJ m^{-2})	Standard deviation (%)	Minimum (MJ m^{-2})	Maximum (MJ m^{-2})	Number of days
2001	G	–	18.48	34.67	1.34	32.49	364
	UV	4.11	0.76	33.99	0.07	1.28	364
	PAR	49.19	9.09	34.13	0.77	15.65	364
	NIR	46.75	8.64	35.62	0.50	15.55	364
2002	G	–	17.64	34.01	1.10	31.21	350
	UV	4.20	0.74	33.47	0.04	1.29	350
	PAR	48.87	8.62	33.71	0.52	15.26	350
	NIR	46.94	8.28	34.65	0.54	14.66	350
2003	G	–	17.82	34.93	2.17	30.82	359
	UV	4.21	0.75	34.21	0.11	1.28	359
	PAR	48.93	8.72	34.51	1.17	14.98	359
	NIR	46.86	8.35	35.72	0.87	14.64	359
2004	G	–	16.85	39.87	1.05	31.43	286
	UV	4.15	0.70	38.16	0.06	1.29	286
	PAR	49.26	8.30	39.45	0.63	15.73	286
	NIR	46.53	7.84	40.82	0.35	14.43	286

description of these parameters in Botucatu was a first step to provide a base for defining data as suspicious. For instance, the data displayed in Fig. 3 and Tables 2 and 3 contain enough information to assess quality of a data measured in any place which climate is similar to Botucatu. Therefore, all values of G, UV, PAR and NIR that diverge considerable from the behavior characterized in Fig. 3 and Tables 2 and 3 were considered suspicious and removed from the analysis.

Due to sensor or data acquisition system malfunctions it was removed 1 day in 2001, 15 days in 2002, 6 days in 2003, 80 days in 2004 and 37 days in 2005.

Observations carried out between 05:30 local time (LST) and 07:30 (LST) and between 17:30 (LST) and 19:30 (LST) were also removed from the dataset due to blocking effects caused by obstacles near to the horizon (Fig. 1). It removed 1431 h of observations carried out in 2001, 1441 h in 2002, 1420 h in 2003, 1771 h in 2004 and 1459 h in 2005.

In this work G, UV, PAR and NIR radiations integrated in 1 h are represented by, H^{h}_{G}, H^{h}_{UV} and H^{h}_{PAR}, and the ones integrated in one day by H^{d}_{G}, H^{h}_{UV}, H^{h}_{PAR} and H^{h}_{NIR}, respectively. Daily values of UV, PAR, NIR and G correspond to the summation of hourly values of UV, PAR, NIR and G. The ratios and averages were estimated from these hourly and daily values.

The criterion to accept the regression model was based on the coefficient of determination R^2, statistically significant at 90% confidence level. The model performances were evaluated using three statistical parameters: MBE (mean bias error), RMSE (root mean square error) and d (index of agreement) [40,49].

3. Results and discussion

3.1. Hourly and daily ratios UV/G, PAR/G and NIR/G

Tables 2 and 3 give the statistical performance of the spectral UV, PAR and NIR components for hourly (Table 2) and daily (Table 3) values respectively. There, the number of hours and days refer to the total period of time when simultaneous measurements of global solar radiation and its two spectral components (UV and NIR) were available in Botucatu.

In general the UV, PAR and NIR ratios of G based on hourly values present little variation from one year to another (Table 2). The UV ratio of G varied from 4.17% (2001) to 4.49% (2004); the PAR ratio of G varied from 48.66% (2003) to 50.00% (2004) and the NIR ratio of G from 46.07% (2004) to 46.88% (2001). For daily values (Table 3), the UV ratio of G varied from 4.11% (2001) to 4.21%

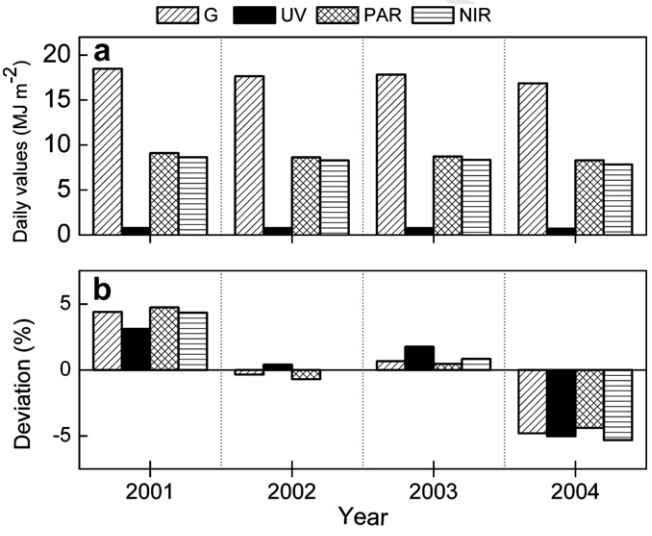

Fig. 4. Time evolution of (a) year-averaged daily values of G, UV, PAR and NIR radiation components and (b) deviation from the mean values of year-averaged daily values observed at the surface in Botucatu from 2001 to 2004.

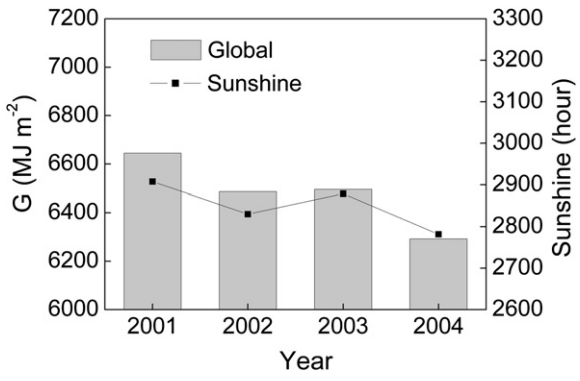

Fig. 5. Time evolution of integrated values of global solar radiation at surface and sunshine hours in Botucatu from 2001 to 2004.

Please cite this article in press as: Escobedo João F, et al., Ratios of UV, PAR and NIR components to global solar radiation measured at Botucatu site in Brazil, Renewable Energy (2010), doi:10.1016/j.renene.2010.06.018

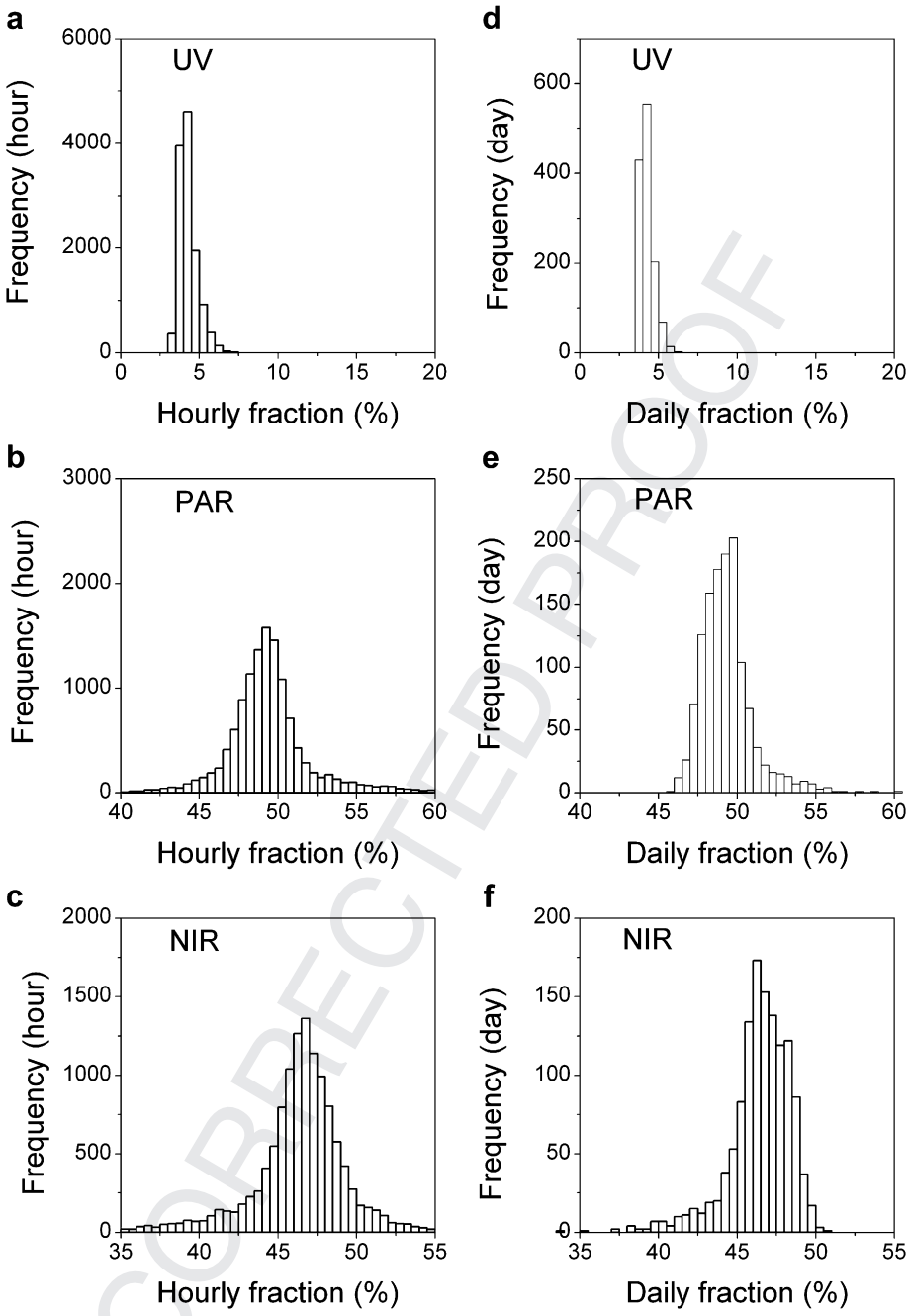

Fig. 6. Histograms of UV, PAR and NIR fractions of G based on (a)–(c) hourly values and ~~(e)~~ (d)–(g) daily values observed at the surface in Botucatu from 2001 to 2004.

(2003); the PAR ratio of G varied from 48.87% (2002) to 49.26% (2004) and the NIR from 46.53% (2004) to 46.94% (2002).

The maximum hourly values of G, UV, PAR and NIR (Table 2) can also be interpreted as the amplitude of the diurnal evolution. G presented a variation from 4.05 MJ m^{-2} (2003) to 4.14 MJ m^{-2} (2002); UV varied from 0.17 MJ m^{-2} (2001 and 2004) to 0.18 MJ m^{-2} (2002 and 2003); PAR varied from 2.03 MJ m^{-2} (2002) to 2.18 MJ m^{-2} (2004) and NIR varied from 1.86 MJ m^{-2} (2004) to 1.97 MJ m^{-2} (2001 and 2002).

Fig. 3 shows the temporal evolution of daily values of G, UV, PAR and NIR spectral components of solar radiation measured in Botucatu, from 2001 to 2004 (Table 3). As expected, the temporal evolution of the three spectral components of global solar radiation matches the evolution of G.

The short term large amplitude oscillations in Fig. 3 occur simultaneously in all spectral components likely is associated with cloud formation in Botucatu. The frequency of cloud in Botucatu is higher during summer and at the end of spring [39,41]. The sunshine hours decrease and the precipitation increases during these seasons in Botucatu (Fig. 2a).

The time evolution of the year-averaged daily values of G, UV, PAR and NIR radiations in Botucatu does not show a large variation (Fig. 4a) and the time evolution of the deviation from the mean value (percentage with respect to the mean value considering the entire period of 2001–2004) indicates that all three spectral components follow also the behavior of G (Fig. 4b). There is no apparent reason for the negative tendency observed for the deviation with respect to the mean in the

Please cite this article in press as: Escobedo João F, et al., Ratios of UV, PAR and NIR components to global solar radiation measured at Botucatu site in Brazil, Renewable Energy (2010), doi:10.1016/j.renene.2010.06.018

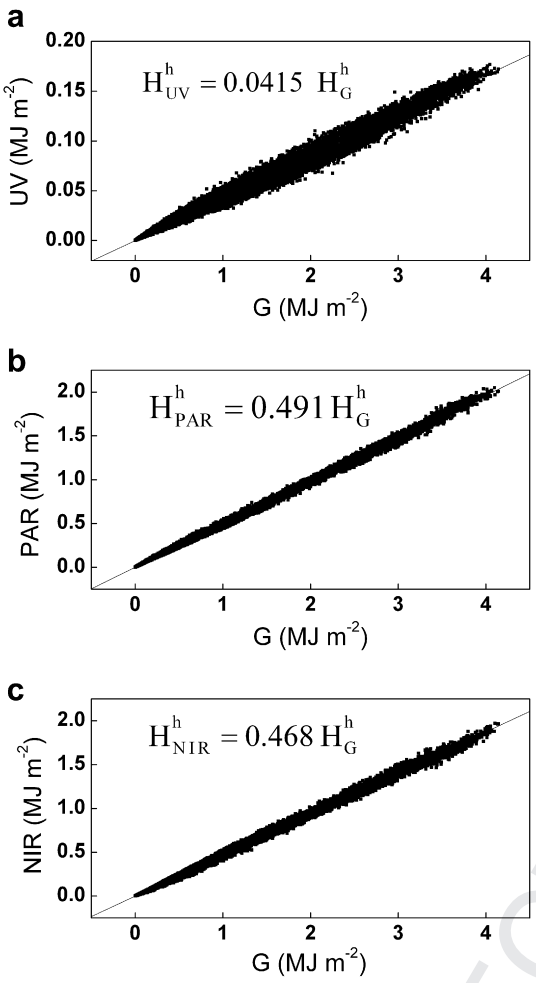

Fig. 7. Scatter plot of hourly spectral irradiances versus global solar radiation (G) for 2001–2004: (a) for UV, (b) for PAR and (c) for NIR.

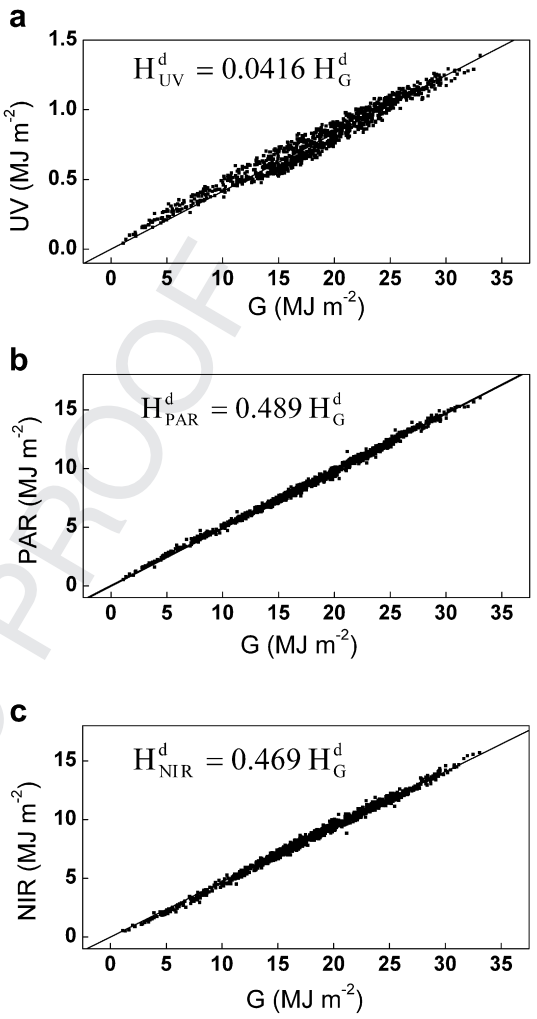

Fig. 8. Scatter plot of daily spectral irradiances versus global solar radiation (G) for 2001–2004: (a) for UV, (b) for PAR and (c) for NIR.

interval 2001–2004 (Fig. 4b). The time evolution of year-integrated global solar radiation at the surface and sunshine in Botucatu (Fig. 5) shows also a negative trend between 2001 and 2004. Any possible effect associated to the missing values in UV, NIR and G that could affect Fig. 4 was reduced in Fig. 5 where year-integrated global solar radiation at the surface and sunshine were estimated from a more complete dataset. Therefore the negative tendency present in Fig. 4 is a real physical response to the interannual increase of nebulosity. The time evolution of the standard deviation for hourly values of G, UV, PAR and NIR oscillated between 50.74% and 56.14% (Table 2). The standard deviation for daily values of G, UV, PAR and NIR oscillated between 33.47% and 40.82% (Table 3).

Fig. 6 shows the frequency distribution of UV, PAR and NIR fractions of G based on hourly and daily values. The hourly fractions varied from 2.8% to 7.0% for UV/G; from 42.7% to 71.0% for PAR/G and from 30.0% to 54.0% for NIR/G. The daily fractions varied from 3.4% to 6.3% for UV/G; from 45.0% to 60.0% for PAR/G and from 34.0% to 51.0% NIR/G. Comparatively, the broader amplitude of hourly fractions occurs because they incorporate short time scale cloudiness variations. The frequency distribution follows a Gaussian distribution and the fractions corresponding to the maximum frequencies (4.25%, 49.25%, 46.75% for hourly and 4.25%, 49.75% and 46.25% for daily values of UV/G, PAR/G and NIR/G) match the mean fractions indicated in Tables 2 and 3.

3.2. Hourly correlation

Fig. 7 shows the correlation between hourly values of G and hourly values of UV, PAR and NIR. The fitting was obtained by linear regression of the observed points forcing the regression line through the origin.

Comparatively the scattering of the points is higher for UV (Fig. 7a) and lower for the PAR (Fig. 7b) radiation. The NIR showed an intermediate behavior (Fig. 7c). The coefficients of determination, $R^2_{PAR} = 0.9978$, $R^2_{NIR} = 0.9968$ and $R^2_{UV} = 0.9794$, indicate that almost 100% of the total variance in PAR, NIR and UV can be explained in terms of the linear relationship existing with G.

One possible explanation for the relatively higher scattering showed by the UV spectral component with respect to G is the difference between the response time of UV and G sensors. While the input signal of the pyranometer that measured G (a

Table 4
Parameters of the hourly linear fits $Y = \alpha X$ for UV, PAR and NIR spectral components.

Expression	R^2
$H^h_{UV} = 0.0415\ H^h_G$	0.9794
$H^h_{PAR} = 0.491\ H^h_G$	0.9978
$H^h_{NIR} = 0.468\ H^h_G$	0.9968

Please cite this article in press as: Escobedo João F, et al., Ratios of UV, PAR and NIR components to global solar radiation measured at Botucatu site in Brazil, Renewable Energy (2010), doi:10.1016/j.renene.2010.06.018

Table 5
Fractions of hourly UV and PAR spectral components to global solar radiation, at different locations.

Ultraviolet fraction of global				
Place	H^h_{UV}/H^h_G(%)	Land use	Latitude, Longitude (degree)	Altitude (m)
Valencia, Spain [32]	2.9	Urban (coastal[a])	39.48°N, 0.38°W	40
Valencia, Spain [33]	3.3	Urban (coastal[a])	39.48°N, 0.38°W	40
Athalassa, Cyprus [51]	3.37	Semi-urban	35.25°N, 33.6°E	165
Granada, Spain [25]	4.0	Rural	37.18°N, 3.58°W	660
Almeria, Spain [25]	3.7	Urban	36.83°N, 2.41°W	0
Botucatu, Brazil	**4.2**	**Rural**	**22.85°S, 48.45°W**	**786**
Córdoba, Spain [26]	4.2	Urban	37.85°N, 4.8°W	125
Valencia, Spain [26]	5.0	Urban (coastal[b])	39.48°N, 0.38°W	20
Kwangju, South Korea [52]	7.7	Urban	35.16°N, 126.88°E	90
Photosynthetically active radiation fraction of global				
Place	H^h_{PAR}/H^h_G(%)	Land use	Latitude, Longitude (degree)	Altitude (m)
Athens, Greece [53]	43.7	Urban	38°N, 24°E	205
Athens, Greece [54]	43.6	Urban	37.10°N, 23.72°E	107
Botucatu, Brazil	**49.0**	**Rural**	**22.85°S, 48.45°W**	**786**

[a] Far sea.
[b] Near sea.

thermocouple) gets stable after 1 s (Table 1), the input signal of the radiometer that measured UV (a photodiode GaP) stabilizes after 5 ms. Therefore, the sensor measuring G will respond to a given input variation at a slow rate compared to the UV sensor. This effect will lag its response and cause a higher scattering of H^h_{UV} in terms of H^h_G, reducing slightly the correlation coefficient. Coefficients lower than 0.98 were also observed for correlation diagrams of H^h_{UV} and H^h_G by Martinez-Lozano et al. [32,33] and Murillo et al. [34]. They all used radiometer model TUVR from Eppley Inc. that uses photoelectric cells to measure UV with response time of the order of milliseconds.

The question arises as to whether absorption/scattering by aerosols has affected the spectral UV portion and consequently the spectral UV/G ratios. Earlier studies showed that the direct solar beam irradiance is strongly affected by the aerosol amount in two ways: the shorter wavelengths (UV band) decrease with increasing aerosol loading, whereas the longer wavelengths increase with increasing aerosol concentration, thus reducing the UV proportions of global solar radiation (G). Nevertheless, spectral investigations support the premise that the aerosols through scattering process incur a significant reduction in the shorter wavelengths, thus affecting the UV band more than the global solar radiation [50]. In addition, scattering processes that may also be enhanced by the sugar cane fires [41] usually observed near Botucatu's site are expected to cause depletion in the spectral UV portion significantly more than in the global solar radiation. Consequently, all these factors may result in a higher data point scatter around the regression line UV = f(G) of Figs. 7a and 8a, reducing further the statistical performance of the regression model in question.

The linear fit expressions obtained from the analysis described above are indicated in Table 4. The slopes of the straight line interpolated by linear regression for hourly values, $H^h_{UV}/H^h_G = 0.0415$; $H^h_{PAR}/H^h_G = 0.491$ and $H^h_{NIR}/H^h_G = 0.468$, match the estimate displayed in Table 2 and the most frequent values in the histograms of Fig. 6a–c.

Based on the literature survey, indicated in decreasing order in Table 5 [25,26,32,33,51,52], the fraction of UV to global solar radiation obtained for Botucatu (4.2%) is higher than the value obtained by Martinez-Lozano et al. [32] and lower than that obtained by Ogunjobi and Kim [52].

Given that water vapor absorbs more G than UV and aerosol attenuates UV more than G, higher UV fraction could be associated to the presence of higher atmospheric water vapor content and lower aerosol load. Valencia, a coastal region, yields values of UV around 3% [32,33] and 5% [26] of G (Table 5). Lower UV ratios (2.9%) in Valencia occurred when observations were carried out far from the Mediterranean Sea (15 km) where the air is drier and the concentration of aerosol is higher. Higher UV fractions occurred when observations were carried near to Mediterranean Sea (0.5 km) where the air is wetter and the concentration of aerosol is lower.

In the case of the PAR spectral component, the hourly values found in the literature, obtained for Athens [53,54] are lower than 49% obtained for Botucatu (Table 5).

3.3. Daily correlation

Correlations between daily values of UV, PAR and NIR and daily values of G (Fig. 8 and Table 6) are similar to hourly correlations (Fig. 7 and Table 4). The scattering of the points is higher for UV (Fig. 8a) and lower for PAR (Fig. 8b) and NIR (Fig. 8c) daily values. The coefficients of determination, $R^2_{PAR} = 0.9904$; $R^2_{NIR} = 0.9870$ and $R^2_{UV} = 0.9204$ are slightly lower than the hourly coefficients values. The slope of the straight lines interpolated by linear regression, $H^d_{UV}/H^d_G = 0.0416$; $H^d_{PAR}/H^d_G = 0.489$; $H^d_{NIR}/H^d_G = 0.469$ do not differ much from their respective hourly counterparts.

Based on the literature survey, indicated in decreasing order in Table 7 [13,20,32,33,51], the fraction of UV to global solar radiation in Botucatu (4.2%) is higher than the lowest value of 2.7% for Valencia, Spain [32] and lower than 5.5% for Corvalis, USA [20].

In the case of the fraction of PAR to global solar radiation, the value found in Botucatu (49%) is higher than most of the reported values in the literature and indicated in Table 7 [13–17,20,24,53,55–57].

The fraction of NIR to global solar radiation in Botucatu (46.9%) is lower than all the values available in the literature and indicated in Table 7 [12,13,36].

3.4. Verification results

To validate the expressions of hourly and daily values of UV, PAR and NIR in terms of G it was used the observations carried out during 2005 in Botucatu.

Table 6
Parameters of the daily linear fits $Y = \alpha X$ for UV, PAR and NIR spectral components.

Expression	R^2
$H^d_{UV} = 0.0416\ H^d_G$	0.9204
$H^d_{PAR} = 0.489\ H^d_G$	0.9904
$H^d_{NIR} = 0.469\ H^d_G$	0.9870

Please cite this article in press as: Escobedo João F, et al., Ratios of UV, PAR and NIR components to global solar radiation measured at Botucatu site in Brazil, Renewable Energy (2010), doi:10.1016/j.renene.2010.06.018

Table 7
Fractions of daily UV, PAR and NIR spectral components to global solar radiation, at different locations.

Ultraviolet fraction of global				
Place	H^d_{UV}/H^d_G(%)	Land use	Latitude, Longitude (degree)	Altitude (m)
Valencia, Spain [32]	2.7	Urban (coastal[a])	39.48°N, 0.38°W	40
Valencia, Spain [33]	3.0	Urban (coastal[a])	39.48°N, 0.38°W	40
Athalassa, Cyprus [51]	3.04	Semi-urban	35.25°N, 33.6°E	165
Botucatu, Brazil	**4.2**	**Rural**	**22.85°S, 48.45°W**	**786**
Tibet Plateau, China [13]	5.3	Mountain	29.68°N, 91.33°E	3688
Corvalis, USA [20]	5.5	Rural	44.57°N, 123.23°W	65.5
Photosynthetically active radiation fraction of global				
Place	H^d_{PAR}/H^d_G(%)	Land use	Latitude, Longitude (degree)	Altitude (m)
Athalassa, Cyprus [57]	42.0	Semi-urban	35.25°N, 33.6°E	165
Athens, Greece [53]	42.9	Urban	38°N, 24°E	205
Lusaka, Zambia [56]	43.6	Biomass burning	15.4°S, 28.3°E	1150
Tibet, China [13]	43.9	Mountain	29.68°N, 91.33°E	3688
San Joaquin Valley, USA [15]	44.9	Rural	36.66°N, 119.5°W	104
Ilorim, Nigeria [17]	45.5	Rural	8.53°N, 4.57°E	375
Corvalis, USA [20]	45.7	Rural	44.57°N, 123.23°W	65.5
Guelph, Canada [14]	47.0	Urban	43.55°N, 80.22°W	334
Athens, Greece [16]	47.3	Urban	37.10°N, 23.72°E	107
Sede Moshe, Israel [55]	47.1	Rural	31.62°N, 34.82°E	130
Jerusalem, Israel, [55]	48.0	Urban	31.78°N, 35.22°E	736
Washington, USA [55]	49.0	Urban	38.9°N, 77°W	22
Rockville, USA [55]	49.0	Urban	39°N, 77.16°W	90
Botucatu, Brazil	**49.0**	**Rural**	**22.85°S, 48.45°W**	**786**
Cambridge, England [24]	50.0	Semi-rural	52°N, 0°E	25
Bet Dagan, Israel [55]	52.1	Urban	32°N, 34.87°E	35
Near infrared radiation fraction of global				
Place	H^d_{NIR}/H^d_G(%)	Land use	Latitude, Longitude (degree)	Altitude (m)
Botucatu, Brazil	**46.9%**	**Rural**	**22.85°S, 48.45°W**	**786**
Campinas, Brazil [12]	49.7%[b]	Urban	22.92°S, 47.08°W	659
Lhasa, China [13]	51.8%	Mountain	29.68°N, 91.33°E	3688
Thule, Northern Greenland [36]	51.0%	Near ice cap	76.40°N, 68.32°W	0

[a] Far sea.
[b] Original value correct by factor 0.92.

Table 8
Mean and standard deviation of *hourly* and *daily* values of G, UV, PAR and NIR observed from 2001 to 2004 and in 2005 at Botucatu.

Period	Radiation component	Hourly		Daily	
		Mean (MJ m^{-2})	Standard deviation (%)	Mean (MJ m^{-2})	Standard deviation (%)
2001–2004	G	1.86	52.14	17.72	35.60
	UV	0.08	51.89	0.74	34.70
	PAR	0.92	52.35	8.70	35.20
	NIR	0.87	52.38	8.29	36.40
2005	G	1.80	51.83	17.07	33.01
	UV	0.07	51.87	0.69	32.47
	PAR	0.90	53.31	8.50	32.99
	NIR	0.83	50.93	7.88	33.50

Comparatively, the mean and standard deviation of hourly and daily values of G, UV, PAR and NIR spectral components observed in the period of time used to derive the model (2001–2004) are similar to the mean and standard deviation of, respectively, hourly and daily values of G, UV, PAR and NIR observed in 2005 (Table 8).

Table 9
Means bias error, root mean square error and index of agreement estimated for the empirical expressions of UV, PAR and NIR in terms of G for hourly and daily.

Model	Radiation component	MBE (%)	RMSE (%)	d
Hourly values	UV	−1.67	9.94	0.993
	PAR	−0.70	4.46	0.999
	NIR	0.90	5.27	0.998
Daily values	UV	−0.66	8.39	0.988
	PAR	−0.57	2.96	0.999
	NIR	0.69	3.73	0.999

Therefore, from the statistical point of view, the dataset used here to validate the linear expressions is compatible with the dataset used to derive them.

The statistical parameters MBE, RMSE and d given in Table 9 correspond to predictions from regression models indicated in Table 4 (hourly) and Table 6 (daily) using data gathered in 2005.

The MBE for hourly values of UV, PAR and UV varied between −1.67% and 0.90%. This interval of MBE variation is of the same order of magnitude of the sensor precision (Table 1). The MBE positive indicates that the model overestimated the hourly values of NIR and underestimated the hourly values of UV and PAR. Similar conclusions can be drawn from the models for daily values of UV, PAR and NIR, with MBE equal to −0.66%, −0.57% and 0.69%, respectively. Lower MBE indicates that the models performed slightly better for daily values.

The hourly values of RMSE are 4.46% for PAR, 5.27% for NIR and 9.94% for UV. The RMSE for daily values are 2.96% for PAR, 3.73% for NIR and 8.39% for UV. Therefore, the models for daily values performed better than the models for hourly values of PAR, NIR and UV spectral components.

The index of agreement close to one indicates that the models performed well for both hourly and daily values of UV, PAR and NIR. The best performance was obtained using model for hourly and daily values of PAR spectral component.

4. Conclusion

The objective of this work was to explore the seasonal evolution of UV, PAR and NIR components of the solar radiation spectrum at the surface and to describe the development and validation of a set of linear regression models to estimate hourly and daily values of

Please cite this article in press as: Escobedo João F, et al., Ratios of UV, PAR and NIR components to global solar radiation measured at Botucatu site in Brazil, Renewable Energy (2010), doi:10.1016/j.renene.2010.06.018

UV, PAR and NIR components of the solar radiation spectrum in terms of hourly and daily values of G observed at the surface.

The data used here corresponds to 5 years of continuous observations of G, UV, and NIR spectral components of the solar radiation, measured simultaneously at the surface with sample rate of 1 Hz and stored as 5-min averaged in the Radiometric Station located in the rural area of Botucatu, country side of the State of São Paulo, Brazil.

In general the UV, PAR and NIR ratios of G based on hourly and daily values present little variation from one year to another. The UV/G varied from 4.11% to 4.49%; the PAR/G varied from 48.66% to 50.00% and the NIR/G varied from 46.07% to 46.94%.

The short term oscillations that occur with large amplitude simultaneously in all spectral components (Fig. 3) are likely to be associated with cloud formation in Botucatu, which is more intense during summer and end of spring.

The time evolution of the year-averaged daily values of G, UV, PAR and NIR radiations in Botucatu does not show a large variation (Fig. 4a). The negative tendency observed for year-averaged daily values of G, UV, PAR and NIR is consistent with the observed variability of cloudiness in the interval 2001–2004.

The scatter plots between UV, PAR and NIR spectral components and G confirmed that they are linearly correlated. The scatter of the points is higher for UV and lower for PAR and NIR. The higher scatter in UV may be associated to the differences in the response time of the UV and G sensors and to the seasonal variation of moisture and aerosol load in the local atmosphere.

The coefficients of determination close to one indicate that most of the variance of UV, PAR and NIR can be explained in terms of the variations of G.

The validation carried out using 1 year of data (2005) indicates that daily and hourly values of PAR, NIR and UV are well estimated with index of agreement near to 1. The PAR spectral component is better estimated than NIR and UV for daily and hourly values.

It should be emphasized that the regression models developed here did not take into consideration the sky conditions. The cloud effects on UV, PAR and NIR spectral components of solar radiation were intensively investigated using the same dataset in ~~Ref.~~ [58]. There, the cloud effect on regression models was objectively estimated in terms of clearness index. As observed in this work, cloud effect is important only for UV models.

Acknowledgments

The authors thank FAPESP, CAPES and CNPq for the financial support for this research.

References

[1] Parisi AV, Wong JCF. An estimation of biological hazards due to solar radiation. Journal of Photochemistry and Photobiology, B: Biology 2000;54:126–30.
[2] Jiménez AE, Estrada CA, Cota AD, Román A. Photocatalytic degradation of DBSNa using solar energy. Solar Energy Materials and Solar Cells 2000;60:85–95.
[3] Jacob DJ. Heterogeneous chemistry and tropospheric ozone. Atmospheric Environment 2000;34:2131–59.
[4] Dodge MC. Chemical oxidant mechanisms for air quality modeling: critical review. Atmospheric Environment 2000;34:2103–30.
[5] Kelly CT, White JR. Photo-degradation of polyethylene and polypropylene at slow strain-rate. Polymer Degradation and Stability 1997;56:367–83.
[6] McCree KJ. Test of current definitions of photosynthetically active radiation against leaf photosynthesis data. Agriculture Meteorology 1972;10:443–53.
[7] Ackerly DD, Bazzaz FA. Seedling crown orientation and interception of diffuse radiation in tropical forest gaps. Ecology 1995;76:1134–46.
[8] Cannel MGR, Grace J. Competition for light: detection, measurement and quantification. Canadian Journal of Forest Research 1993;23:1969–79.
[9] Baldocchi D, Hutchinson B, Matt D, Mcmitten R. Seasonal variations in the radiation regime within oakhickory forest. Agricultural and Forest Meteorology 1984;33:177–91.
[10] Frisina VA. Modelagem das radiações global, difusa, e fotossinteticamente ativa em ambiente protegido e suas relações com o crescimento e produtividade da cultura de pimentão [*Capsicum annuum* L.] Botucatu-SP. School of Agronomic Sciences, State University of São Paulo, Botucatu, São Paulo, Brazil, 156 pp (in Portuguese).
[11] Larsen NF, Stamnes K. Use of shadows to retrieve water vapor in hazy atmospheres. Applied Optics 2005;44:6986–94.
[12] Pereira AR, Machado EC, de Camargo MBP. Solar radiation regime in three cassava (Manihot sculenta Grantz) canopies. Agricultural Meteorology 1982;26:1–10.
[13] Zhang X, Zhang Y, Zhoub Y. Measuring and modelling photosynthetically active radiation in Tibet Plateau during April–October. Agricultural Meteorology 2000;102:207–12.
[14] Blackburn WJ, Proctor JTA. Estimating photosynthetically active radiation from measured solar irradiance. Solar Energy 1983;31:233–4.
[15] Howell TA, Meek DW, Hatfield JL. Relationship of photosynthetically active radiation to shortwave radiation in the San Joaquin Valley. Agricultural Meteorology 1983;28:157–75.
[16] Papaioannou G, Papanikolaou N, Retalis D. Relationships of photosynthetically active radiation and shortwave irradiance. Theoretical and Applied Climatology 1993;48:23–7.
[17] Udo SO, Aro TO. Global PAR related to solar radiation for central Nigeria. Agricultural and Forest Meteorology 1999;97:21–31.
[18] Alados I, Foyo-Moreno I, Alados-Arboledas L. Photosynthetically active radiation: measurements and modelling. Agricultural and Forest Meteorology 1996;78:121–31.
[19] Stigter CJ, Musabilha MM. The conservative ratio of photosynthetically active to total radiation in the tropics. Journal of Applied Ecology 1982;19:853–8.
[20] Rao CRN. Photosynthetically active components of global solar radiation: measurements and model computations. Archives for Meteorology, Geophysics, and Bioclimatology 1984;34:353–64.
[21] Britton CM, Dodd JD. Relationships of photosynthetically active radiation and shortwave irradiance. Agricultural Meteorology 1976;17:1–7.
[22] Ting KC, Giacomelli GA. Availability of solar photosynthetically active radiation. Transactions of the Asae 1987;6:121–32.
[23] Karalis JD. Characteristics of direct photosynthetically radiation. Agricultural and Forest Meteorology 1989;48:225–34.
[24] Szeicz G. Solar radiation for plant growth. Journal of Applied Ecology 1974;11:617–36.
[25] Foyo-Moreno I, Vida J, Alados-Arboledas L. A simple all weather model to estimate ultraviolet solar radiation (295–385 nm). Journal of Applied Meteorology 1999;38:1020–6.
[26] Cañada J, Pedros G, Bosca JV. Relationships between UV (0.290–0.385 μm) and broad band solar radiation hourly values in Valencia and Córdoba, Spain. Energy 2003;28:199–217.
[27] Al-Aruri S, Rasas M, Al-Jamal K, Shaban N. An assessment of global UV solar radiation in the range (0.290–0.385 μm) in Kuwait. Solar Energy 1988;41:159–62.
[28] Elhadidy MA, Abdel-Nabi DY, Kruss PD. Ultraviolet solar radiation at Dhahram (Saudi Arabia). Solar Energy 1990;44:315–9.
[29] Koronakis PS, Sfantos GK, Paliatsos AG, Kaldellis JK, Garofalakis JE, Koronakis IP. Interrelations of UV-global/global/diffuse solar irradiance components and UV-global attenuation on air pollution episode days in Athens, Greece. Atmospheric Environment 2002;36:3173–81.
[30] Khogali A, Al-Bar OF. A study of solar ultraviolet radiation at Makkah solar station. Solar Energy 1992;48:79–87.
[31] Feister U, Grasnick KH. Solar UV radiation measurements at Potsdam. Solar Energy 1992;49:541–8.
[32] Martinez-Lozano JA, Casanovas AJ, Utrillas MP. Comparison of global UV (290–385 nm) and global irradiation measured during the warm season in Valencia, Spain. International Journal of Climatology 1994;14:93–102.
[33] Martinez-Lozano JA, Tena F, Utrillas MP. Ratio of UV to global broad band irradiation in Valencia, Spain. International Journal of Climatology 1999;19:903–11.
[34] Murillo W, Cañada J, Pedrós G. Correlation between global ultraviolet (290–385 nm) and global irradiation in Valencia and Cordoba (Spain). Renewable Energy 2003;28:409–18.
[35] Robaa SM. A study of ultraviolet solar radiation at Cairo urban area, Egypt. Solar Energy 2004;77:251–9.
[36] Bolsenga SJ. Near infrared radiation in Northern Greenland. Journal Applied Meteorology 1997;6:449–51.
[37] Oliveira AP, Escobedo JF, Machado AJ, Soares J. Diurnal evolution of solar radiation at the surface in the City of São Paulo: seasonal variation and modeling. Theoretical and Applied Climatology 2002;71:231–49.
[38] Oliveira AP, Escobedo JF, Machado AJ, Soares J. Correlation models of diffuse solar radiation applied to the City of São Paulo (Brazil). Applied Energy 2002;71(1):59–73.
[39] Assunção FH, Escobedo JF, Oliveira AP. Modelling frequency distributions of 5 minute-averaged solar radiation indexes using Beta probability functions. Theoretical and Applied Climatology 2003;75:213–24.
[40] Soares J, Oliveira AP, Boznar MZ, Mlakar P, Escobedo JF, Machado AJ. Modeling hourly diffuse solar radiation in the city of São Paulo using neural network technique. Applied Energy 2004;79:201–14.
[41] Assunção FH, Escobedo JF, Oliveira AP. A new algorithm to estimate sky condition based on 5 minutes-averaged values of clearness index and relative optical air mass. Theoretical and Applied Climatology 2007;90:235–48.

Please cite this article in press as: Escobedo João F, et al., Ratios of UV, PAR and NIR components to global solar radiation measured at Botucatu site in Brazil, Renewable Energy (2010), doi:10.1016/j.renene.2010.06.018

[42] Codato G, Oliveira AP, Soares J, Escobedo JF, Gomes EN, Pai AD. Global and diffuse solar irradiances in urban and rural areas in southeast of Brazil. Theoretical and Applied Climatology 2008;93:57–73.
[43] Assis FN, Mendez MEG. Relação entre radiação fotossinteticamente ativa e radiação global. Pesquisa Agropecuaria Brasileira 1989;24:797–800 [in Portuguese].
[44] França S, Bergamaschi H, Rosa LMG. Modelagem do crescimento de milho em função da radiação fotossinteticamente ativa e do acúmulo de graus-dia, com e sem irrigação. Revista Brasileira de Agrometeorologia 1999;7:59–66 [in Portuguese].
[45] Assunção HF, Escobedo JF. Modelo e medida da irradiância solar ultravioleta em Botucatu. Energia Na Agricultura 2005;20:29–46 [in Portuguese].
[46] Jacovides CP, Steven MD, Asimakopoulos DN. Solar spectral irradiance under clear skies around a major Metropolitan area. Journal of Applied Meteorology 2000;39:917–30.
[47] WMO. Revised instruction manual on radiation instruments and measurements. In: Frölich Claus, London Julius, editors. WCRP Publications series No. 7, WMO/TD No. 149. World Climate Research Progaramme (WRCP) WMO/ICSU Joint Scientific Committee; October 1986. p. 134.
[48] Fröhlich C, London J. Revised Instruction manual on radiation instruments and measurements. In: WCRP Publications series No. 7. WMO/TD No. 149; October 1986.
[49] Willmott CJ. On the validation of models. Physical Geography 1981;2:184–94.
[50] Jacovides CP, Tymvios FS, Asimakopoulos DN, Kaltsounides NA, Theoharatos GA, Tsitouri M. Solar global UVB (280–315 nm) and UVA (315–380 nm) radiant fluxes and their relationships with broadband global radiant flux at an eastern Mediterranean site. Agricultural and Forest Meteorology 2009;149:1188–200.
[51] Jacovides CP, Assimakopoulos VD, Tymvios FS, Theophilou K, Asimakopoulos DN. Solar global UV (280–380 nm) radiation and its relationship with solar global radiation measured on the island of Cyprus. Energy 2006;31:2728–38.
[52] Ogunjobi KO, Kim YJ. Ultraviolet (0.280–0.400 μm) and broadband solar hourly radiation at Kwangju, South Korea: analysis of their correlation with aerosol optical depth and clearness index. Atmospheric Research 2004;71:193–214.
[53] Jacovides CP, Tymvios FS, Assimakopoulos VD, Kaltsounides NA. The dependence of global and diffuse PAR radiation components on sky conditions at Athens, Greece. Agricultural and Forest Meteorology 2007;143:277–87.
[54] Papaioannou G, Nikolidakis G, Asimakopoulos D, Retalis D. Photosynthetically active radiation in Athens. Agricultural and Forest Meteorology 1996;81:287–98.
[55] Stanhill G, Fuchs M. The relative flux density of photosynthetically radiation. Journal of Applied Ecology 1977;14:317–22.
[56] Finch DA, Bailey WG, Mcarthur LJB, Nasitwitwi M. Photosynthetically active radiation regimes in a southern African savanna environment. Agricultural and Forest Meteorology 2004;122:229–38.
[57] Jacovides CP, Timvios FS, Papaioannou G, Asimakopoulos DN, Theofilou CM. Ratio of PAR to broadband solar radiation measured in Cyprus. Agricultural and Forest Meteorology 2004;121:135–40.
[58] Escobedo JF, Gomes EN, Oliveira AP, Soares J. Modeling hourly and daily fractions of UV, PAR and NIR to global solar radiation under various sky conditions at Botucatu, Brazil. Applied Energy 2009;86:299–309.

Please cite this article in press as: Escobedo João F, et al., Ratios of UV, PAR and NIR components to global solar radiation measured at Botucatu site in Brazil, Renewable Energy (2010), doi:10.1016/j.renene.2010.06.018